Predictive heuristic control

Inferring risks from heterogeneous nowcast accuracy

van der Werf, Job Augustijn; Kapelan, Zoran; Langeveld, Jeroen Gerardus

DOI
10.2166/wst.2023.027

Publication date
2023

Document Version
Final published version

Published in
Water science and technology : a journal of the International Association on Water Pollution Research

Water Science & Technology

© 2023 The Authors Water Science & Technology Vol 87 No 4, 1009 doi: 10.2166/wst.2023.027

Predictive heuristic control: Inferring risks from heterogeneous nowcast accuracy

Job Augustijn van der Werf[a,*], Zoran Kapelan[a] and Jeroen Gerardus Langeveld[a,b]

[a] Section of Sanitary Engineering, Water Management Department, Faculty of Civil Engineering and Geosciences, Delft University of Technology, Delft, The Netherlands
[b] Partners4UrbanWater, Nijmegen, The Netherlands
*Corresponding author. E-mail: j.a.vanderwerf@tudelft.nl

JAvdW, 0000-0001-6768-7829; ZK, 0000-0002-0934-4470; JGL, 0000-0002-0170-6721

ABSTRACT

Urban Drainage Systems can cause ecological and public health issues by releasing untreated contaminated water into the environment. Real-time control (RTC), augmented with rainfall nowcast, can effectively reduce these pollution loads. This research aims to identify key dynamics in the nowcast accuracies and relate those to the performance of nowcast-informed rule-based (RB)-RTC procedures. The developed procedures are tested in the case study of Rotterdam, the Netherlands. Using perfect nowcast data, all developed procedures showed a reduction in combined sewer overflow volumes of up to 14.6%. Considering real nowcast data, it showed a strong ability to predict if no more rain was expected, whilst performing poorly in quantifying rainfall depths. No relation was found in the nowcast accuracy and the consistency of the predicted rainfall using a moving horizon. Using the real nowcast data, all procedures, with the exception of the one predicting the end of the rainfall event, showed a significant risk of operative deterioration (performing worse than the baseline RB-RTC), linked to the relative performance of the nowcast algorithm. Understanding the strengths of a nowcast algorithm can ensure the reliability of the RB-RTC procedure and can negate the need for detailed modelling studies by inferring risks from nowcast data.

Key words: combined sewer overflows, rainfall forecast, real-time control, risk assessment, urban drainage systems

HIGHLIGHTS

- Rainfall nowcast inclusion in control procedures should be preceded by a careful risk analysis.
- Nowcast accuracy is highly heterogenous, meaning the applicable for control varies.
- Nowcast accuracy can be used to qualify the risk associated with the implementation of control.
- Predicting the end of the event was found to be the most reliable predictive ability, with limited performance loss due to uncertainties.

GRAPHICAL ABSTRACT

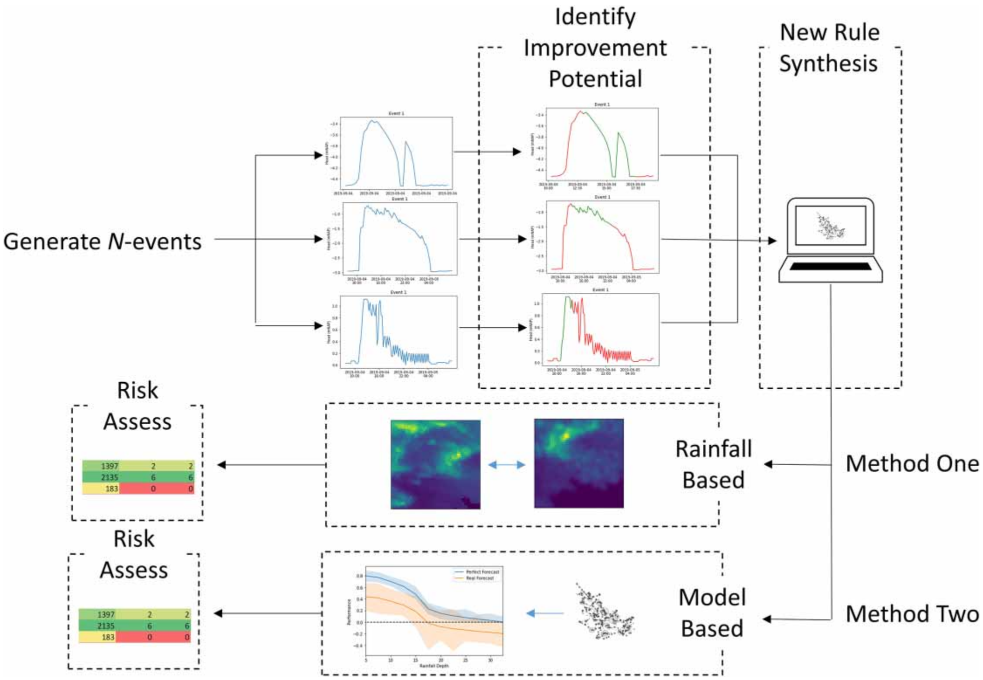

1. INTRODUCTION

Urban areas are expanding globally, concentrating waste streams and negatively impacting the natural environment. Overloading of existing urban drainage systems (UDS) through densification of existing areas, urbanisation of surrounding areas and climate change can increasingly lead to combined sewer overflows (CSOs) and urban flooding (Mahaut & Andrieu 2019), which negatively impact the receiving water bodies and public health (Ten Veldhuis *et al.* 2010; Botturi *et al.* 2020; Owolabi *et al.* 2022). To mitigate this problem, (blue-green) infrastructure expansion is often used as a solution but can be too expensive or impossible to implement due to space constraints. Real-time control (RTC) aims to use real-time information about the system-state to optimally operate the UDS (Schütze *et al.* 2002) and thereby reduce the impact on the receiving water bodies (Langeveld *et al.* 2013) without the need for large-scale infrastructure investments. Implementation of these operative optimisation practices is becoming increasingly widespread, aided by their inclusion in the new Urban Wastewater Treatment Directive of the European Union (European Commission 2022).

The way in which the set-points (the target setting of each controlled actuator) of the actuators are determined (the procedure as per the nomenclature set by Schütze *et al.* (2002)) can be classified as either heuristic or real-time optimisation control (García *et al.* 2015). Although there is some theoretical evidence that real-time optimisation can outperform heuristic control (Lund *et al.* 2018), the additional efforts required for this type of control can outweigh the operational performance of the UDS (Beeneken *et al.* 2013; Mollerup *et al.* 2017). Consequentially, despite the numerous publications on real-time optimisation methods, heuristic control strategies remain the most ubiquitously applied version of RTC for UDS, as published examples on implemented real-time optimisation procedures, in practice, remain scarce (van der Werf *et al.* 2022). The lack of implemented examples and therefore uncertainty about the practical performance of predictive-based control procedures remains one of the main barriers against real-time optimisation control implementation (Naughton *et al.* 2021). Integrating forecasts within existing heuristic control procedures, under the principle of nowcast-informed RTC, could provide the missing link needed towards the widespread implementation of more advanced forms of RTC.

The influence of nowcast uncertainty has been shown to be negligible in real-time optimisation procedures (Fiorelli *et al.* 2013; van der Werf *et al.* 2023). This is attributed to the continuous updating of the model (when using model-predictive control), forecasts and a discount factor. Rule-based RTC (RB-RTC) strategies, as applied in practice, typically function with predefined set-points and thresholds embedded in suitable *if-then* operation rules (García *et al.* 2015). These RB-RTC methods

Table 1 | Overview of the performance of predictive RB-RTC cited in literature

Reference	RTC objective	Forecast horizon	Performance increase with forecast in RTC
Gaborit *et al.* (2012)	TSS removal	72 h	66% compared to no forecast
Gaborit *et al.* (2016)	TSS removal	24 h	42% compared to no forecast
Bilodeau *et al.* (2019)	Maximum peak flow from storm drain[a]	3 h	43% reduction in maximum peak flow
Ibrahim (2020)	Maximum peak flow from the basin	Not specified	56.2%

[a]It should be noted that this is one of the criteria assessed, which is found to be most comparable to CSO reduction.

can be augmented with prediction, showing an increase in the efficacy of RB-RTC potential. Before expanding this form of control with nowcast or long-term forecasts, the prediction accuracy and potential associated risks should be considered. In previous work, the efficacy of this nowcast-informed RB-RTC strategy has been shown to work well for single detention ponds or storm drains (Table 1). The application of nowcast-informed RB-RTC for CSO reduction in combined sewer systems, however, has not been studied to the same extent compared to detention ponds and storm drains.

Importantly, nowcast accuracy (the ability to correctly predict the rainfall over a given horizon) is not homogeneous and depends on the rainfall characteristics (Lin *et al.* 2005; Fabry & Seed 2009; Imhoff *et al.* 2020). The effects of these heterogeneities in nowcast accuracy on UDS modelling and consequently the RTC efficacy have not been explicitly considered in existing forecast-induced uncertainty studies (Achleitner *et al.* 2009; Schellart *et al.* 2014; Löwe *et al.* 2016) where uncertainty is commonly modelled using the homogeneous Gaussian noise (Pleau *et al.* 2001; Svensen *et al.* 2021). This can lead to inaccurate conclusions being drawn on the influence of nowcast uncertainty on the performance of RTC strategies and should therefore be avoided.

Therefore, this paper aims to develop efficient, nowcast-informed RB-RTC strategies and to assess if there are risks associated with heterogeneous nowcast accuracy. Furthermore, it aims to assess if these risks can be directly inferred from nowcast and rainfall data.

2. METHODOLOGY

To establish the potential influence of rainfall nowcast accuracy on the performance of nowcast-informed heuristic control procedures, a methodology comprising of several steps has been developed (Figure 1). Firstly, rainfall data (nowcast and observed) is obtained and discretised into separate rainfall events, followed by the creation of a RB-RTC procedure without the use of nowcast (as a baseline). Then, the potential for operational performance improvement of the UDS through improved control measures is established (Section 2.1). Sets of new rules are consequently developed, each utilising specific aspects of the rainfall forecast (e.g. the predicted end of the rainfall event or storage capacity exceedance), to capture the potential heterogeneous nature of forecast accuracy. These sets of rules form the new nowcast-informed RB-RTC procedure. The performance using both perfect and real rainfall forecasts is then assessed and, if relevant, the risk of performance loss related to these rules is quantified (Section 2.2). This is done by only looking at the forecast accuracy (Section 2.2.1) or using a model-based approach to quantify the risk (Section 2.2.2). A qualitative comparison of the findings obtained from both methods is then made and relevant conclusions are drawn (Section 2.3).

2.1. Performance improvement assessment and new rule synthesis

Firstly, available nowcast and observed rainfall datasets have to be obtained. Here, the observed rainfall dataset is a rain-gauge-adjusted radar product, following a data assimilation procedure detailed by Overeem *et al.* (2009). The nowcast data is an open-source product obtained using an advection model based on real-time observation of two C-bands operated by the Royal Netherlands Meteorological Institute (KNMI, see dataplatform.knmi.nl). The rainfall datasets obtained this way then have to be discretised into individual rainfall events to allow for an event-based risk assessment (using the methodology set out in Section 2.3). Here, the definition of a rainfall event uses a minimum inter-event time (MIT) of 12 h based on the rain-gauge-adjusted radar product, recommended as this is the approximate emptying time of the system (Joo *et al.* 2013).

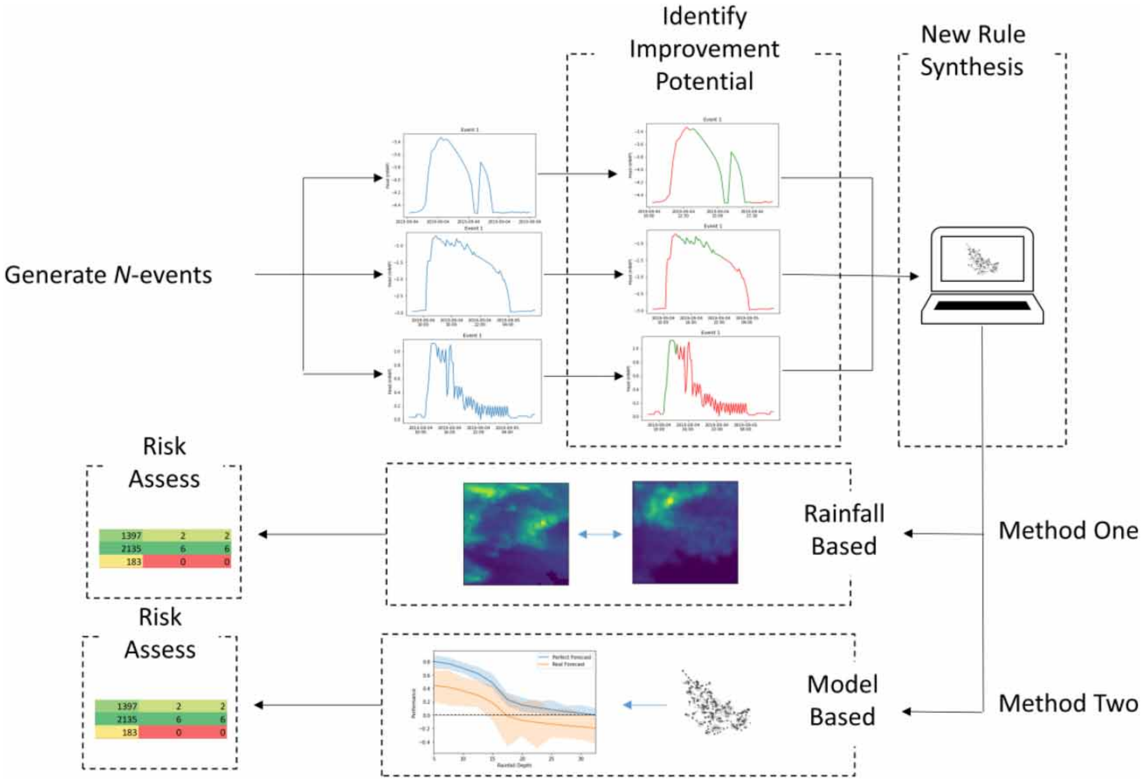

Figure 1 | Overview of the steps in the methodology. First, events are defined and the models and rainfall are generated. Performance improvement is then assessed, followed by the synthesis of a new, nowcast-informed RB-RTC procedure. The functioning of these procedures is assessed following a model-based and a rainfall-based method. The associated risks are compared in a qualitative manner.

The nowcast data, which is provided in dBZ (see, for example, Imhoff *et al.* 2022), has to be converted to rainfall data. This is done using the following empirically derived equation (Marshall *et al.* 1955):

$$I = 10^{\frac{Z-109}{32}} \quad (1)$$

where I is the precipitation intensity in mm/hr and Z is the reflectivity factor observed in dBZ.

Before the RB-RTC procedure through the inclusion of nowcast is considered, an analysis of the potential of RTC-based operational improvement has to be done, relative to existing UDS operation without nowcast. Using the previously established rainfall events, the model-based performance evaluation methodology presented by van Daal *et al.* (2017) is followed to determine the current functioning of the RTC. For the same events, the adjusted absolute central basin approach (aCBA), previously used in the computation of performance indicators (van der Werf *et al.* 2021), is used to compute the maximum performance potential of the UDS through RTC, while the former indicates the current performance of the UDS. The adjusted aCBA computes the maximum achievable performance of the current UDS configuration by the iteratively lumping pumped section into a single basin with the aim to compute the minimum CSO volume theoretically possible (see Supplementary Material section 1 (Extended Methodology and Figure S1) for a more detailed breakdown of this previously developed method).

Rainfall events are then ranked based on the difference between the predicted performance and the maximum achievable performance. Events with the largest difference are analysed by first identifying the location and timing of the CSO events. Then, the settings of the actuators influencing the CSO location are analysed before, during and after the CSO event. Potential improvements are noted by using the expert judgement of the dynamics of the system and by assessing the filling degrees in the UDS up- and downstream of an activated in combination with actuator settings to see if local improvements could have been realised.

Based on this performance improvement potential, updated rules expanding on the existing heuristic RTC procedure are developed. Here, the existing RB-RTC is updated into a nowcast-informed RB-RTC through two types of rule augmentations: (1) nowcast-based bifurcations at the existing rules (where *if-then* logic is added to the current *if-then* rule) and (2) replacement of the existing rules by outputs of a nowcast-forced model. To assess the effect of potential nowcast accuracy heterogeneity, the nowcast-informed RB-RTC should include augmentations at different phases (beginning, during and at the end of the rainfall event) and based on different rainfall properties (total depth or intensity).

The implementation of the control rules can either be (1) nowcast-based heuristic control or (2) model-informed heuristic control. Nowcast-based heuristic control directly uses the nowcast data within the RB-RTC procedure (e.g. if predicted rainfall depth <0.5 mm, then pump-off). Conversely, the model-informed heuristic control uses the nowcast as rainfall forcing in the (simplified) model of the UDS, making the RB-RTC procedure dependent on the filling degree predicted through the UDS model. In the model-informed heuristic control procedure, the monitoring data available is used to generate the initial conditions of the model, and the available nowcast data is thereafter used as the forcing of the model. Every set of updated nowcast-informed rules is implemented and simulated separately (see Sections 2.2.1 and 2.2.3 for the assessment methodologies used).

The rules for perfect nowcast data (using the observed rainfall) are developed following a heuristic approach, relying on UDS understanding rather than formal optimisation to develop and calibrate the rules. This form of rule generation was deemed sufficient as long as the operational performance with respect to the control objective of the nowcast-informed RB-RTC using perfect prediction was higher compared to the baseline RB-RTC.

2.2. Nowcast RB-RTC risk assessment

Two types of risks associated with various forms of uncertainties in a real-time optimisation context were previously identified: (1) risk of UDS performance loss and (2) risk of operational deterioration of UDS. The former indicates a decreased improvement compared to the perfect prediction scenario, but a net increase in UDS operational performance compared to a baseline, and the latter means a loss of performance compared to the baseline, induced by operational uncertainties.

To assess these potential risks, two methods are compared: (1) assessing the accuracy of the nowcast dependent on features (related to, for example, the depth or stage of the rainfall) used in the RB-RTC procedure and (2) comparing the model-informed performance using real nowcast data as the input of the RB-RTC procedure. The first method does not require UDS nor RTC modelling and is, therefore, the preferred method. The validity of this method, however, can only be established if the risks are first calculated through a model-based risk assessment, the methodology which is further expanded in Section 2.2.2. Therefore, the two methods are compared here to assess if the same conclusions can be drawn in which case the forecast-based risk assessment would be preferred; otherwise, the model-based risk assessment has to be used.

2.2.1. Forecast-based risk assessment

To assess if there is heterogeneity in the nowcast accuracy, several key properties are considered, keeping the nature of the use of the nowcast within the RB-RTC procedure in mind. The key properties assessed for heterogeneity in accuracy are (1) accuracies dependent on the stage of the rainfall event (start, middle or end), (2) accuracy dependent on forecast horizon, (3) forecast consistency and its relation to accuracy and (4) accuracy dependent on total rainfall depth. These key properties are further explained below.

As the prediction horizon used in this work (2 h) is significantly smaller than the MIT (12 h), sub-events are discretised from the larger events, with the sub-MIT set to 3 h (thereby keeping no-rain time periods within the assessed data).

2.2.1.1. Depth and binary prediction. Various metrics have been used in the performance evaluation of radar rainfall nowcasting techniques (Ashok & Pekkat 2022). In the nowcast-informed RB-RTC procedure, the forecast-induced bifurcations are frequently dependent on a pre-set, stationary threshold. For this reason, the rain-gauge-adjusted and nowcast datasets are transformed into binary datasets using multiple thresholds to get a set of binary datasets in combination with the numerical predictions. For every updated prediction in the dataset, the sum of the forecasted rainfall over the horizon is compared to the threshold, with the exceedance of the threshold amounting to a *True* and non-exceedance to a *False*. This will give an insight if the predictability of events depends on the rainfall depth. The same procedure is applied to the rain-gauge-adjusted dataset using the same forecasting horizon. To assess the strength of the binary predictions, both the probability of detection (POD) and specificity (SPC) are estimated as follows:

$$\mathrm{POD} = \frac{\mathrm{TP}}{\mathrm{TP} + \mathrm{FN}} \tag{2}$$

$$\mathrm{SPC} = \frac{\mathrm{TN}}{\mathrm{TN} + \mathrm{FP}} \tag{3}$$

where TP is the number of true positives (correctly predicted *True* values), FN is the number of false negatives (wrongly predicted *True* values), TN is the number of true negatives (correctly predicted *False* values) and FP is the number of false positives (wrongly predicted *False* values).

2.2.1.2. Temporal heterogeneity. Temporal heterogeneity in the forecast accuracy refers to the ability of the nowcast algorithm's ability to predict the dynamics at the start, during or end of a rainfall event. To assess this heterogeneity, two discretisation techniques are used: time-dependent and depth-dependent discretisation. In the former, each rainfall event is discretised in 10 equal parts with the same duration of the event and the latter follows a 10 equal part discretisation using the total rainfall depth to discretise the event (see Figure 2). The POD and SPC are computed at every stage and used to generate a distribution of POD and SPC values. Both Kolmogorov–Smirnov (KS) and Anderson–Darling (AD) two-sample tests are used to assess if the distributions differ significantly (for each discretised part of the rainfall event). Given the relative power at the centre and tail of the two tests, respectively (Baumgartner & Kolassa 2021), significant results from both tests would most accurately represent potential changes in risk (through the tail-heavy analysis of the AD two-sample test) and overall efficacy (through the centre-heavy analysis of the KS two-sample test), which used to assess if these distributions differ (for each discretised part of the rainfall event). The adjacent distributions of POD and SPC values are compared and assessed for statistically significant ($p < 0.05$) differences.

2.2.1.3. Forecast horizon influence. The negative influence of the increasing forecasting horizon on the nowcast accuracy has previously been shown (Achleitner *et al.* 2009). To deal with this in a real-time optimisation setting, a discount factor, used to change the relative importance of current performance to future performance, is commonly employed (Vezzaro & Grum 2014; Tian *et al.* 2022). From a heuristic control perspective, the understanding of the accuracy over the prediction

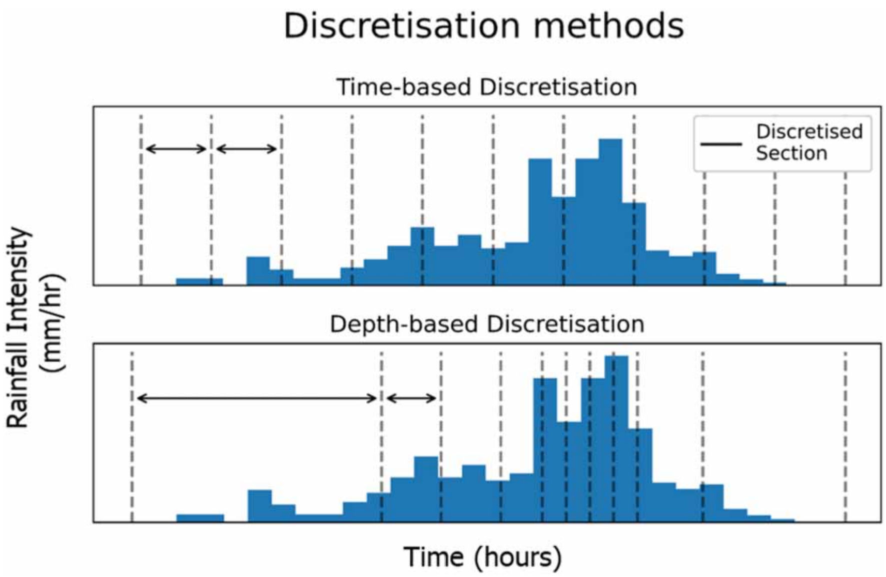

Figure 2 | Difference between the time-based and depth-based discretisation methods. For the depth-based method, the cumulative depth is used to generate 10 sections with equal total rainfall depths. The rainfall event shown here is a synthetic event of arbitrary length and intensity.

horizon can influence the horizon used within the RB-RTC. Here, at every updated prediction, the cumulative prediction over the available 5-min increments is compared to the rain-gauge-adjusted radar data using the following root-mean-square error (RMSE):

$$\mathrm{RMSE}_T = \sqrt{\frac{\sum_{i=1}^{N}\left(\sum_{t=0}^{T} x_{i,t} - \sum_{t=0}^{T} \hat{x}_{i,t}\right)}{N}} \tag{4}$$

where the RMSE_t is the root-mean-square error deviation for the horizon of length T, $x_{i,j}$ is the ith rain-gauge-adjusted rainfall at time-step t within the prediction horizon, $\hat{x_{i,t}}$ is the ith predicted rainfall at time-step t within the prediction horizon and N is the total number of samples in the dataset. The change in the RMSE of the cumulative predicted rainfall is assessed here to better understand if the summation over the horizon allows for a self-correcting mechanism, or if an increased deviation is observed (as per the individual predictive strength evaluated by Imhoff *et al.* (2020)).

2.2.1.4. Nowcast consistency. The level of nowcast consistency refers to the level of change in the given sub-section of the nowcast as the model is continuously updated. To assess this, a sub-section of the data (in this case half of the forecast horizon) is tracked as it approaches the moment of implementation (see Figure 3 on the left). At the point of implementation in the RB-RTC performance point, the tracked windows are assessed using a correlation coefficient matrix, and the final level of nowcast consistency is defined as the mean value of the lower triangular matrix, excluding the correlation matrix diagonal (see Figure 3 on the right). A negative relation between the mean correlation and the nowcast RMSE over the $0 - n$ horizon is assumed here.

The risks associated with the inclusion of different nowcast attributes cannot be directly inferred from the statistical methods described previously, given the non-linear nature of RTC performance to rainfall characteristics (Vezzaro 2021). For this reason, a model-based risk assessment method is needed to quantify the risk associated with the nowcast accuracy properties assessed.

2.2.2. Model-based risk assessment

Two previously defined risks, the risks of performance loss and operational deterioration, related to the various analysed aspects of the nowcast rainfall data, need to be computed. To achieve this, the updated procedures shown in Section 2.1 are implemented in the EPA StormWater Management Model (SWMM) 5.1 software (Rossman 2015) through the PySWMM python interface (McDonnell *et al.* 2020). To gain a better understanding of the performance and its dynamics,

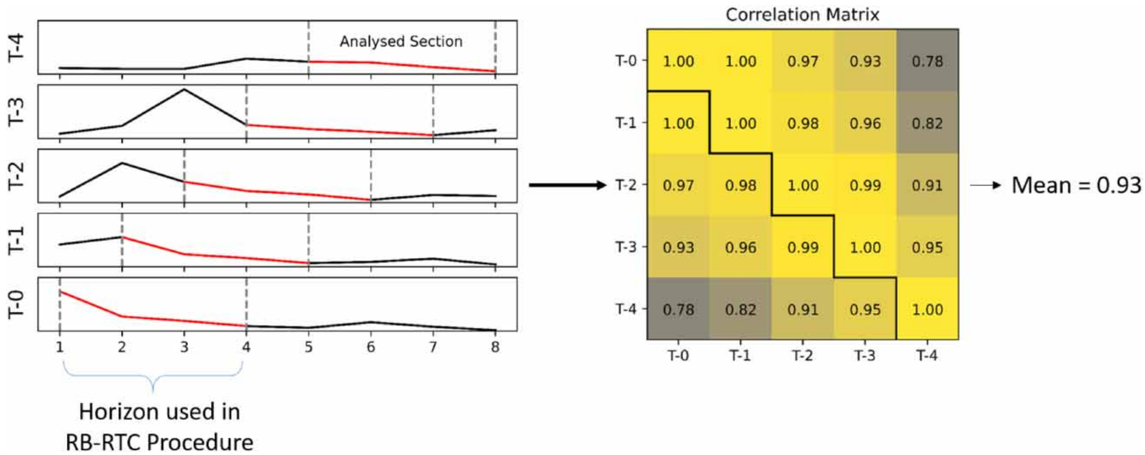

Figure 3 | Method used for the assessment of prediction consistency. A sub-section of the nowcast data is selected and tracked, and a mean value of a part of the correlation matrix (below the black line in the figure on the right) is calculated as a way to quantify the consistency. The *x*-axis indicates the number of time steps included, here a time-step represents 15 min, resulting in a horizon of 2 h in total.

reading of the SWMM output files is done through the python SWMM API (Pichler 2022). Both full hydrodynamic (FH) and simplified models can be used for the model-based risk assessment, providing adequate model calibration has been conducted. Here, a simplified model of the case study UDS was used, given the too-inhibitive computational inefficiency associated with FH models.

With the new rules implemented, *N*-rainfall events representative of the spread of rainfall characteristics typical for the used case study are simulated using the aforementioned SWMM model. The number of rainfall events used depends on the available data and computational efficiency of the used SWMM model, noting that it is recommended to use multiple years of data where possible (van Daal *et al.* 2017). Each simulation is done using the observed rainfall as the nowcast data (perfect forecast) and another using real nowcast data available in real time through the KNMI for RTC purposes. The perfect and real forecast outputs are then compared to the established baseline (the RB-RTC procedure set-up prior to the inclusion of nowcast data). The aforementioned risks of performance loss and operative deterioration associated with each set of nowcast-informed RB-RTC procedures are then calculated by comparing the performances in two simulations with the baseline RB-RTC performance.

2.3. Risk assessment comparison

The *a priori* implications determined through the nowcast-based risk assessment (Section 2.1) are compared to the model-based risk assessment method. As the risk of operational deterioration and performance loss are directly quantified through the model-based risk assessment and the nowcast-based risk assessment has to infer these based on various nowcast metrics, the comparison between the two methods cannot be directly quantitative. The operational risks (both operational deterioration and performance loss) related to each set of nowcast-informed rules, determined through the model-based risk assessment, are therefore ranked first (from highest to lowest risk). This ranking is then compared to the relative performance of the nowcast property associated with the nowcast-informed rules to see if a high risk is associated with a relatively poor performance in nowcast accuracy.

3. CASE STUDY

The methodology was applied to the part of the City of Rotterdam, the Netherlands, which discharges into wastewater treatment plant (WWTP) Dokhaven. WWTP Dokhaven has a design capacity of 560,000 p.e. and serves the southern and western parts of Rotterdam. CSOs in the cities discharge to either the urban canals or the Nieuwe Maas, a river discharging in the North Sea and forming the basis for the Port of Rotterdam. CSOs discharging in the urban canals cause significantly more ecological and public health issues compared to those discharging in the Nieuwe Maas. The UDS consists of 61 different sewer districts, totalling an impervious area of 1,632 ha. These districts are connected through pumps in a cascading layout. The UDS is located in a flat area, with a total storage capacity of 10.13 mm (designed using a 1-in-2-year rainfall event) and is fitted with eight pumped CSOs discharging in the Nieuwe Maas, enabling controlled CSO discharges (to minimise discharges into the local environment). The approximate locations of the CSOs and the distribution of the sewer districts are shown in Figure 4.

The new heuristic control was set up as a part of CAS (Central Automatic Control) 2.0 project and details set-points for 52 pumping stations (including the pumped CSOs) in the catchment. The development and implementation of the used model and baseline RB-RTC (upon which the nowcast rules were developed here) were done as part of the aforementioned CAS2.0 project, as described in Langeveld *et al.* (2022). The key logic in the CAS2.0 RB-RTC procedure is a change in set-points of pumping stations (by either partially switching the pumps off to protect downstream districts or switching the pumped CSOs on), which is dependent on the upstream and downstream filling degrees (using a 80% filling degree (FD) as the set threshold). A graphical representation displaying this main logic is shown in Figure 5.

The set-points for each of the pumping stations are derived in a central computer after receiving the relevant information from the water level and flow sensors from the UDS and the WWTP. These set-points are then sent to the programmable logic controllers at each pumping station, which use the new set-point as a target achieved following a local control algorithm. This allows for a distributed implementation of the central control, overcoming difficulties with complicated, unreadable codes.

The control strategy was set up as a multi-objective problem, aiming to reduce the frequency and volume of CSO discharges to the urban canals first, then the total CSO volume and finally the reduction of overloading the WWTP. As no formal real-time optimisation algorithm was used, a hierarchical form of control objective, namely the reduction of CSO volumes

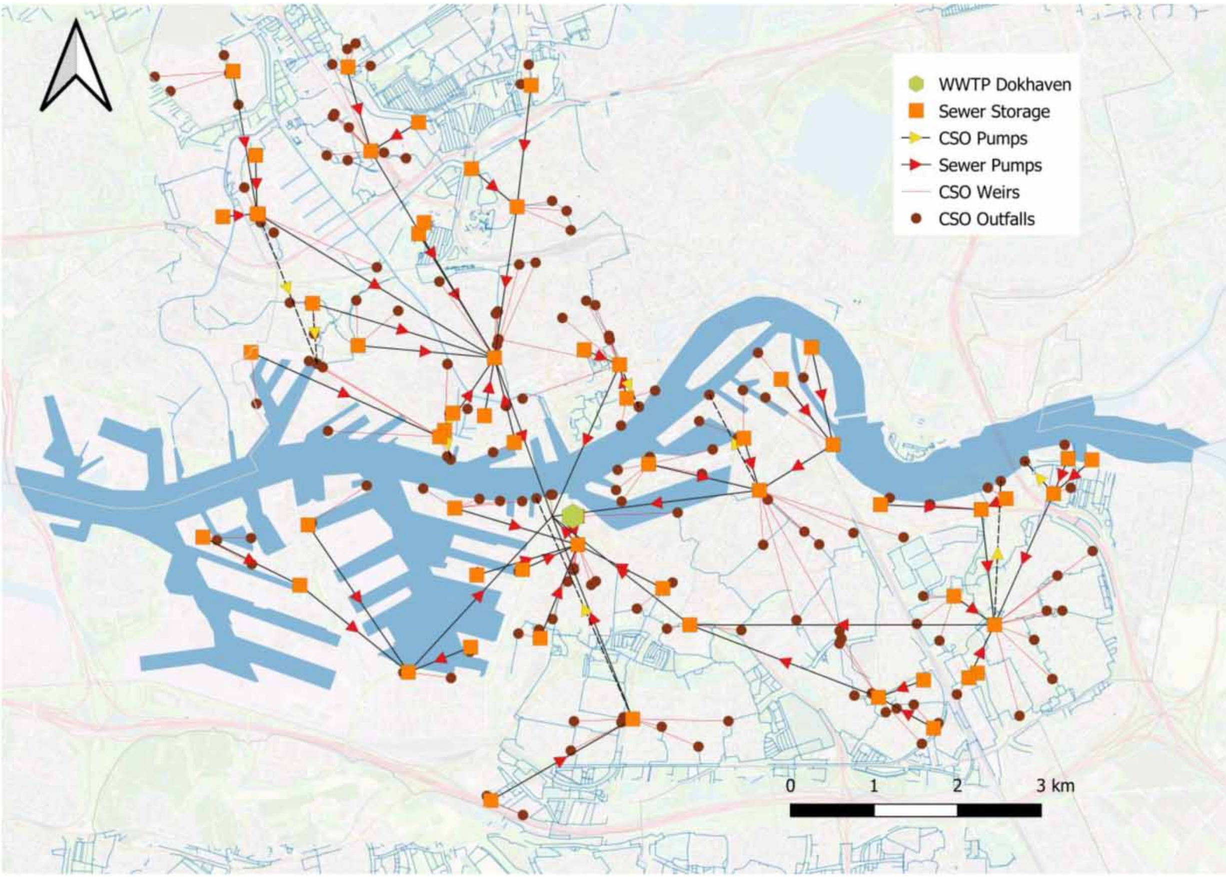

Figure 4 | Schematic map of the sewer system connected to the Dokhaven Wastewater Treatment Plant.

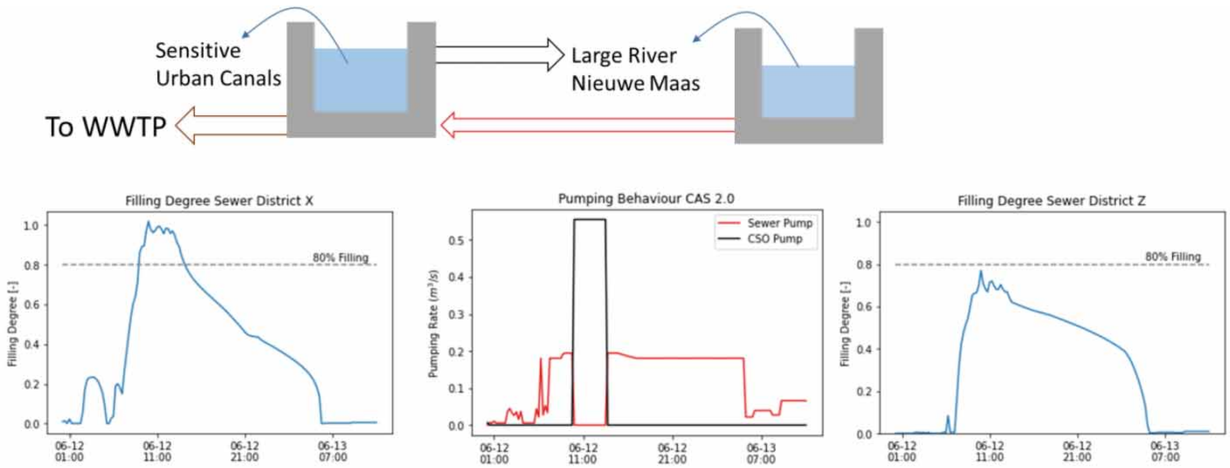

Figure 5 | Representation of the main logic driving the heuristic rules of the CAS 2.0 project. It aims at protecting the urban canals by the reduction of inflow towards areas discharging into those canals and utilising CSO pumps to further decrease the discharge into the canals. This is at the expense of the Nieuwe Maas, a busy shipping river in the city of Rotterdam.

discharged to the urban canals, was used as opposed to a weighted CSO volume synthesis (as proposed by Vezzaro & Grum (2014)). When reporting the results, the total CSO volume is used as means to indicate the improvement of the system performance, unless an increase in the CSO volume towards the urban canals has been caused.

Due to physical constraints of the pumping station configurations, the minimum sampling interval of the pumps (the time between adjusting the pumping station set-points) is 15 min. This sampling interval is, therefore, used within the model-based risk assessment.

The shown schematisation of the UDS (Figure 4) is used to build the simplified simulation model, with each sewer district modelled as a reservoir and the storage curve and hydrological data (for each sewer district) based on a previously calibrated model used for the development of the CAS2.0 RB-RTC procedure (Langeveld *et al.* 2022). The storage curve is derived from the full hydrodynamic model of the sewer districts. CSOs in each district are implemented and the depth of the flow curve is derived from full hydrodynamic model data. The existing RTC rules are augmented using six different sets of new rules (i.e. new RTC procedures), utilising nowcast data in different ways (Table 2). Given the presence of the CSO pumps, some of the nowcast-informed rules apply only to these actuators (RTC procedure 1). The other RTC procedures make the operation of all pumping stations in the original RB-RTC using different total depths for activation (RTC Procedures 3 and 5), event phases (RTC Procedures 1 and 2), spatially aggregated data (RTC Procedure 6) or fully relying on the nowcast and current data within the established RB-RTC (Procedure 4). More details including examples of the developed procedures can be found in the Supplementary Materials (Section 2 and Figures S2–S7).

To assess the updated RB-RTC performance, 95 rainfall events with reliable data for both the nowcast and rain-gauge-adjusted datasets were identified within the available dataset (2020–2021 period). The individual rainfall events were identified using the MIT of 12 h. These contain rainfall events with return periods of up to 2 years (Figure 6).

4. RESULTS

4.1. Operational performance potential

The potential for performance improvement compared to the baseline RB-RTC was assessed for the 95 events previously described. Based on the results obtained using the aCBA method, a total CSO volume reduction of 37.2% was possible through optimal operation of the UDS when compared to the baseline. For rainfall events with a smaller total rainfall depth, complete preventions of CSOs have been achieved. For larger rainfall events, the maximum CSO volume reduction was 5.8%. This is consistent with previous results, showing the highest potential of RTC impact in the events with low- to mid-rainfall depths (van der Werf *et al.* 2022).

4.2. Forecast accuracy and risks

4.2.1. Rainfall depth

The predictive ability to correctly predict larger rainfall events is significantly lower compared to smaller rainfall depths (Figure 7). The POD value drops from 0.93 for predictive ability above 0.25 mm to around 0.5 when the threshold is set

Table 2 | Description of the updated rules, including the relevant nowcast properties used in the rule, used to assess the impact of nowcast uncertainty on the efficacy of the improved RB-RTC procedure

New RTC procedure ID	RB-RTC type	Nowcast properties	Description
1	Nowcast-based heuristic control	End of event predicted	If the end of an event is detected, the CSO pumps are switched off
2	Nowcast-based heuristic control	End of the event predicted	If the end of an event is detected, the entire system switches back to <80% FD conditions
3	Model-informed heuristic control	Total predicted volume throughout the event	Following the RB-RTC rules when exceedance of 0% FD is predicted
4	Model-informed heuristic control	Total predicted volume throughout the event	Following the RB-RTC rules when exceedance of 80% FD is predicted
5	Model-informed heuristic control	Tracked hour in advance	Following the RB-RTC rules when exceedance of the 90% FD threshold was exceeded for at least half of the predictions in the tracked hour
6	Model-informed heuristic control	Tracked hour over connected upstream and downstream catchments	Following the RB-RTC rules when exceedance of the 80% FD threshold was exceeded for the district or the upstream or the downstream districts for at least half of the predictions in the tracked hour

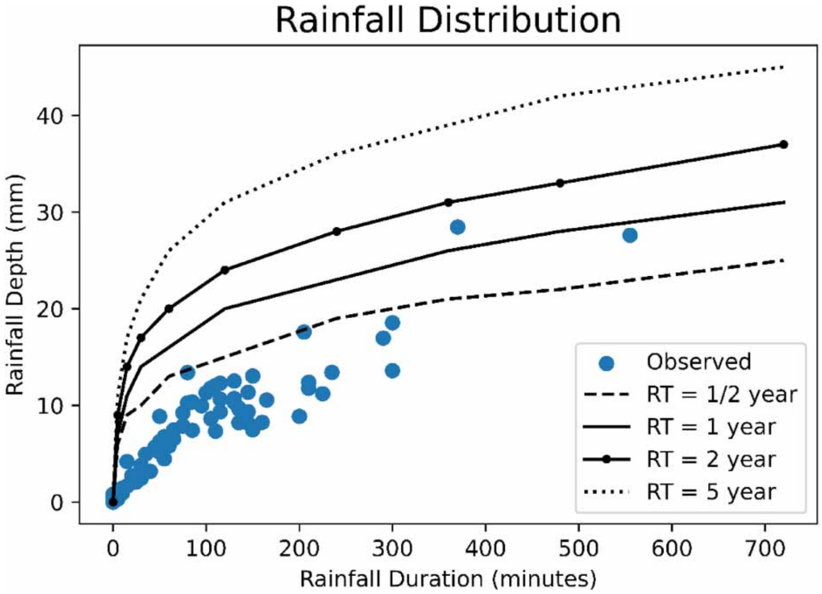

Figure 6 | Distribution of the rainfall events in the dataset compared to the relevant rainfall statistics (based on Beersma *et al.* 2019).

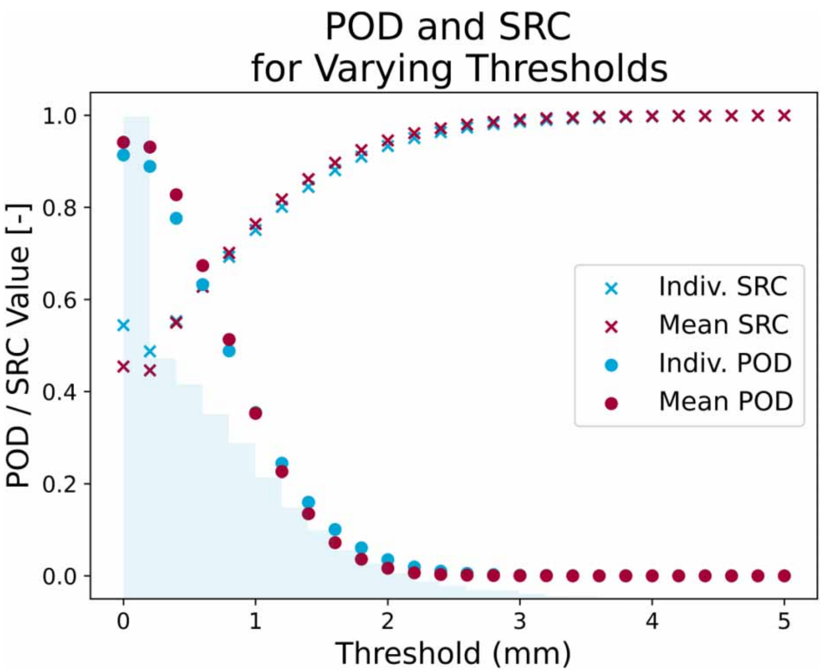

Figure 7 | Detail of the POD and SPC values for different threshold rainfall depths over two horizons. The histogram displays the relative abundance in the dataset per threshold interval. No significant difference is found when a spatial mean of the predicted rainfall is used rather than individual pixels.

to 1 mm of cumulative predicted rainfall. This drops further to a POD value of 0.1 for any threshold above 5 mm. The SPC, on the other hand, increases during the same interval, ending in a maximum value of 0.98 for the larger rainfall events. The abundance of data points is significantly higher for the lower fractions partially due to the discretisation method of the rainfall events (using an MIT of 12 h).

These results suggest a negative bias within the nowcast dataset, as an underestimation of the real rainfall would see a rise in SPC and a drop in POD with an increasing threshold used. This is in line with previous research showing a decreased ability to predict large (often convective) rainfall events (e.g. Foresti *et al.* 2016; Pulkkinen *et al.* 2020). This has also been shown to lead to decreased discharge forecast abilities (Imhoff *et al.* 2022) for hydrological models, conclusions which can largely be extrapolated to the UDS.

4.2.2. Forecasting horizon

The range of the error (difference between the predicted and observed rainfall) increases close to linearly with the increase in the length of the forecast horizon (Figure 8). The frequency of overestimation is slightly higher, with a mean difference of −0.03 mm and the absolute value of the 25% confidence interval (CI) being larger than the 75% CI (−1.1 and 0.62 mm, respectively). Considering the 5–95% CI, however, the errors indicate an opposite trend, whereby the nowcast underestimates the larger, observed values (−2.3 and 4.1 mm, respectively). This implies potentially reduced control potential through nowcast inclusion when directly using the cumulative values, particularly when relatively large volumes are predicted (mainly at the start and during a rainfall event). Considering the mean difference over the catchment (using the mean of the cumulative rainfall over all the pixels, see Figure 8(a)), a similar trend can be observed, although the relatively large underestimations do seem to have smoothened out when considering spatial means. Despite the wide range in pixel value difference in the 5–95% CI range, the 25–75% CI bands could be small enough to have meaningful potential in a UDS control strategy and the mean difference is close to zero (indicating the absence of a clear bias).

The RMSE in the cumulative rainfall prediction (see Figure 6(b)), however, increases exponentially when considering the individual pixel predictions (i.e. the input to any UDS model used in a model-predictive sense). This is in line with the previous exponential decrease in Pearson's correlation as reported by Imhoff *et al.* (2020).

4.2.3. Nowcast consistency

A decreasing trend in the distribution of the total RMSE was observed when comparing the total rainfall forecast for an hour horizon with the mean correlation coefficient (used as a metric for the nowcast consistency), as shown in Figure 9. This was expected, as a consistent nowcast was assumed to be more reliable. However, when using a normalised RMSE (normalisation by division with the total observed rainfall), no such relation could be seen. The normalised data for the highest consistency

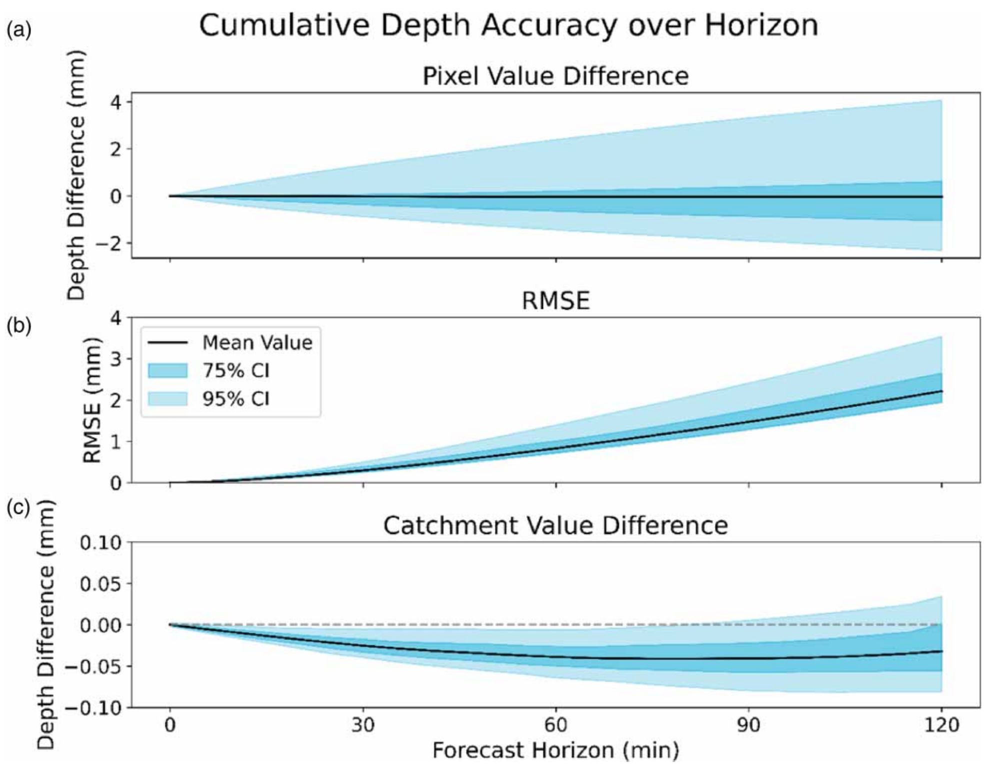

Figure 8 | Evolution of the uncertainty of the cumulative rainfall depth over the full prediction horizon available (120 min).

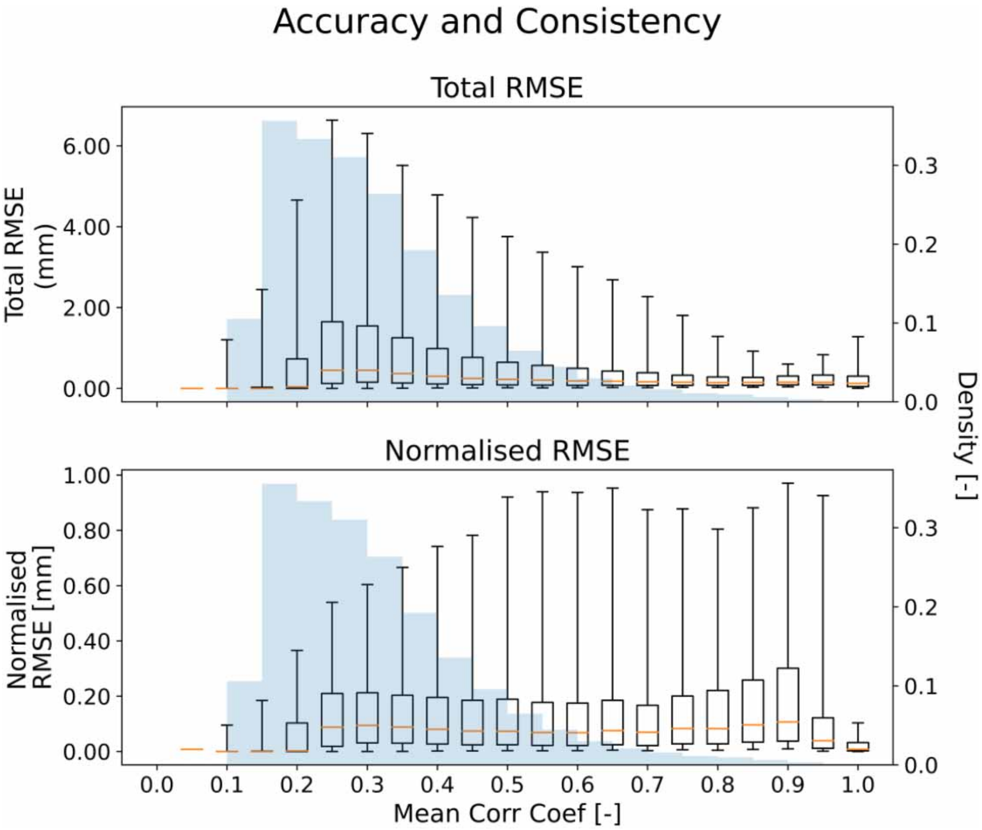

Figure 9 | Analysis of the consistency of the nowcast compared to the nowcast. The boxplot indicates the RMSE value and the normalised RMSE value for the upper and lower plots, respectively, per interval of 0.05 of the mean correlation coefficient. The blue histogram plots the relative occurrence of that interval within the dataset. Whiskers indicate the 5–95% CI. Please refer to the online version of this paper to see this figure in colour: http://dx.doi.org/10.2166/wst.2023.027.

(0.95–1.0) has a significantly improved distribution, particularly due to the number of no-rain forecasts within this subset (which have relatively high predictability). Furthermore, the dataset shows a higher density in the 0.1–0.4 mean correlation coefficient interval. The highest quarter (0.75–1.0) of the mean correlation coefficient only accounts for 2.35% of the total dataset. Statistically significant recommendations based on the relation between accuracy and consistency can, therefore, not be made. From a control perspective, the additional benefit of only using the nowcast if a certain mean correlation coefficient is reached cannot be asserted from this data. However, given the lack of a relation between the mean correlation coefficient and the normalised RMSE, it can be assumed that there is little merit in the use of a control procedure based on the tracking of nowcast consistency. The reduction of the nowcast horizon from 120 to 60 min within the RB-RTC will likely have a larger impact on the performance due to the relatively increased predictive capacity (see Figure 8) rather than through the tracking mechanism.

A stronger link between the mean correlation coefficient and the depth of the rainfall event was found. The consistency of the nowcast for 0–0.5 mm of rainfall in the forecasted hour was significantly higher ($p < 0.05$) compared to other intervals. This relationship explains the difference between the normalised RMSE and the total RMSE shown in Figure 9, as the higher end of the mean correlation coefficient is dominated by low rainfall data (thus having a relatively low RMSE but no difference in normalised RMSE).

4.2.4. Temporal heterogeneity

Strong statistical evidence ($p < 0.01$ following the KS two-sample test and $p < 0.01$ following the AD two-sample test) indicates an improved ability of the prediction at the tail end of the rainfall event, in both the POD and SPC distributions, following a time-based discretisation method (Figure 10(a)). This shift is dominated by a reduction in the relative prevalence

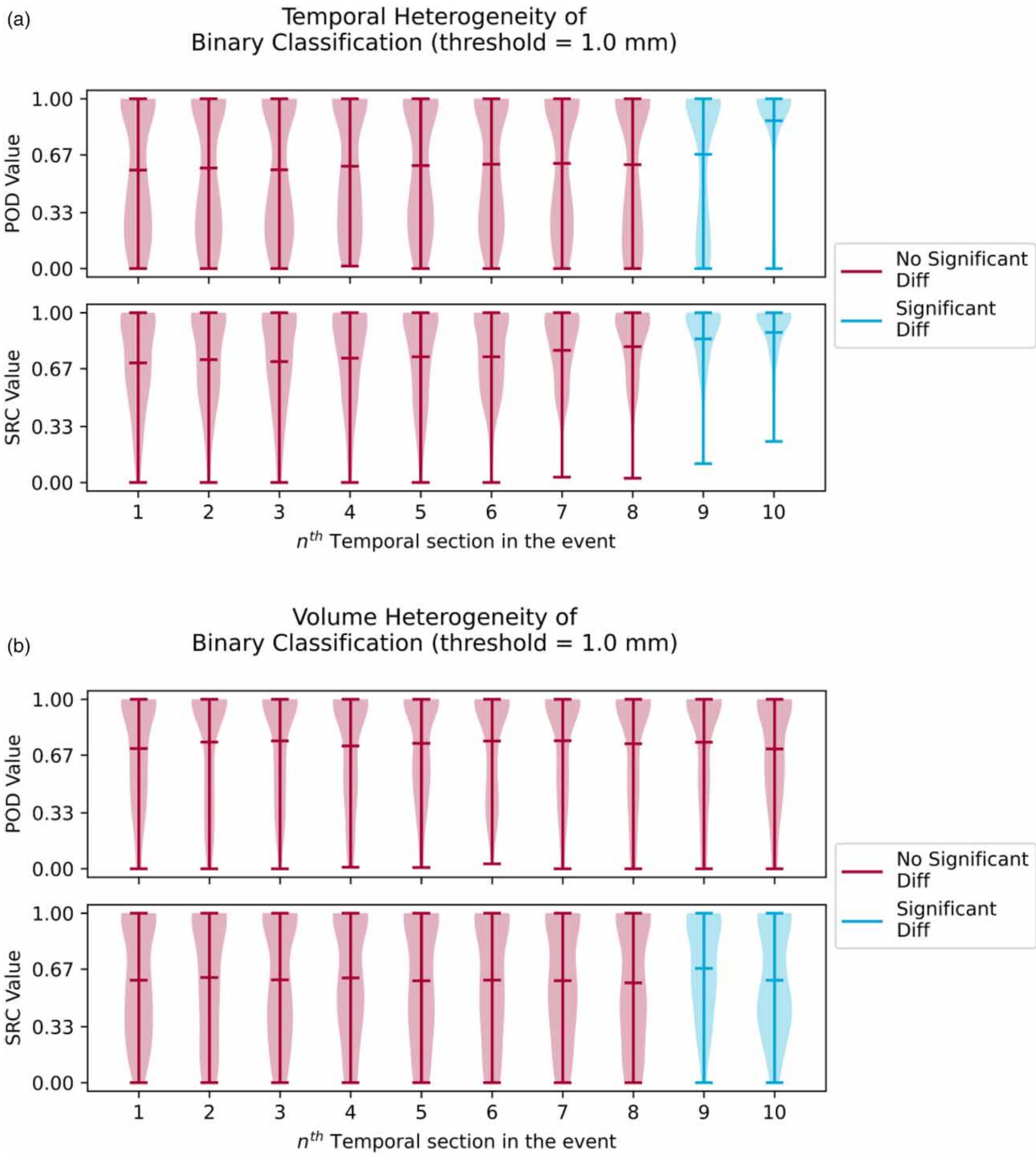

Figure 10 | Results of the temporal discretisation of the rainfall event following either (a) a time-based or (b) volume-based discretisation methods. Blue distributions indicate significant difference from the previous distribution. Please refer to the online version of this paper to see this figure in colour: http://dx.doi.org/10.2166/wst.2023.027.

of lower values (0–0.5). Particularly the relative improvement in the SPC distribution (assessing the ability to correctly predict the *False* (no rainfall) values) indicates a good ability to assess if an event has ended. Interestingly, the opposite effect was observed for the volume-based sampling method, with a statistically significant reduction in the SPC performance ($p < 0.05$ for the KS two-sample test and $p < 0.02$ for the AD two-sample test) for the tail end of the rainfall events (Figure 10(b)).

From a control perspective, the time-based discretisation method gives a more accurate representation of the end of the event, as the volume-based method forces the inclusion of rainfall data. The implementation of *end-of-event logic* (i.e. switching off CSO pumps when no more rain is expected) will follow the time-based implementation, meaning that this form of control is unlikely to be strongly affected by nowcast-induced errors.

4.3. Model-based risk assessment

Using the simplified UDS simulation model, the performance of the updated RB-RTC procedures was assessed. When the perfect nowcast data is used, all the updated procedures outperform the baseline RB-RTC (Figure 11), with a limited risk of operational deterioration. In this case, RTC Procedure 4 showed the highest total CSO volume reduction potential (14.6% or 10.5 mm), followed by Procedure 3 (12.9% or 9.3 mm), Procedure 2 (10.9% or 7.8 mm), Procedure 6 (10.6%, 8.1 mm), Procedure 1 (9.8%, 7.1 mm) and Procedure 5 (8.7%, 6.9 mm). Despite this decrease in total CSO volume, a risk of operational deterioration (i.e. the existence of an event with worse performance compared to the baseline) was present for all updated RTC procedures except Procedure 1. However, the minor increases in CSO frequency and total volumes in Procedures 2–6 were offset in all cases by the corresponding gains made through the updated RB-RTC procedures resulting in the negation of small events.

However, when the real nowcast data is used, a considerable risk of both performance loss and operational deterioration is noted for all updated RB-RTC procedures (Figure 11). Only two RTC procedures (Procedures 1 and 2) reduced the total CSO volume of the operation under the real nowcast scenarios but significantly less compared to the theoretical potential (Table 3). Procedures 4 and 6 show a minor increase in the CSO reduction compared to the baseline (both 0.8%). However, most notably, Procedures 3 and 5 show a net increase in the total CSO volume of 17.7 and 15.7%, respectively. In the case of Procedure 3, this increase in volume is predominantly caused by the pumped CSOs being activated unnecessarily, as shown in Figure 11 as the column on the low part of the baseline performance. As a result, 40.8% of the events within the dataset had a worse performance compared to the baseline RB-RTC. Procedure 5 also resulted in a number of events with deteriorated UDS operation (25.0%), but the relative CSO increase was caused less by the unnecessary CSO pumping and more by a decreased performance throughout all the rainfall events.

RTC of UDS aims to utilise the existing UDS optimally by ensuring the optimal distribution of runoff throughout the system. Consequentially, if there is a failure throughout the system (i.e. nowcast inaccuracies), the possibility of adverse effects increases. The two control systems which had the highest performance decrease (Procedures 3 and 5) were both designed to (1) use the numerical output of the nowcast algorithms directly and (2) operate closer to the total filling of the UDS. No relation between the apparent risk and the RTC potential (i.e. the performance using the perfect data) was found.

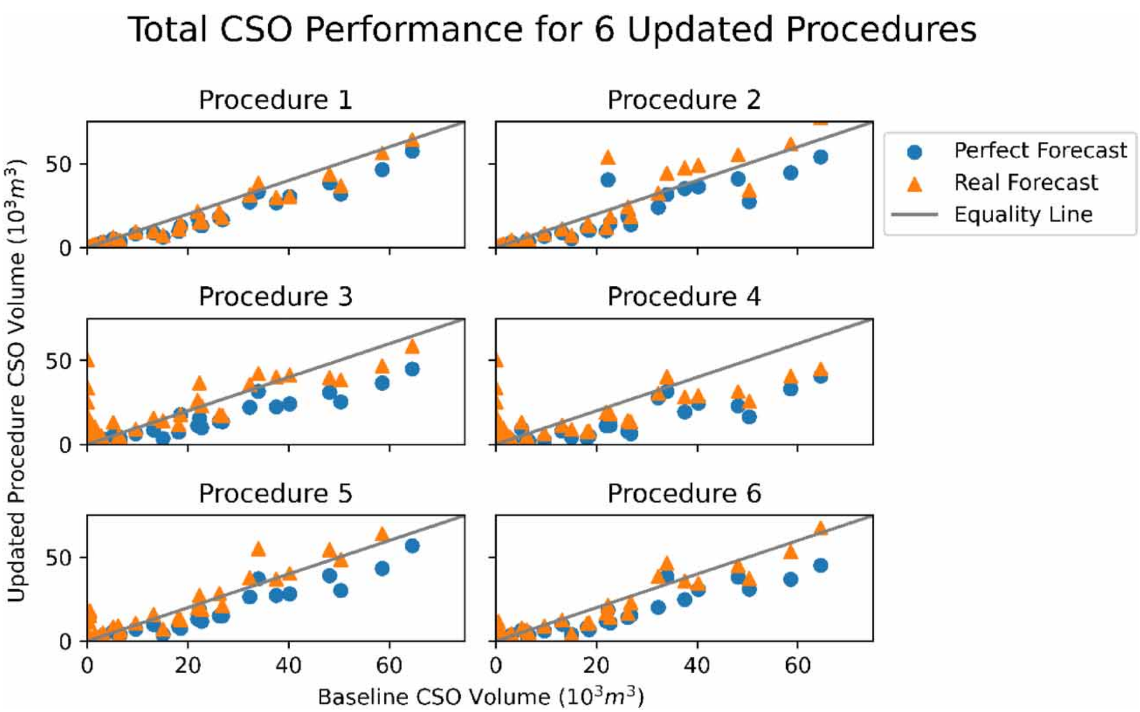

Figure 11 | Performance overview for the six updated RB-RTC procedures, considering both perfect and real nowcast data.

Table 3 | The performance of the six procedures compared to the baseline, a relative increase to the perfect nowcast data and the frequency of deterioration (total CSO volume higher than the baseline RB-RTC results)

RTC procedure ID	CSO volume reduction relative to baseline RB-RTC	Increase in CSO volume compared to perfect nowcast (%)	Percentage of rainfall events with deteriorated operation relative to perfect nowcast (%)
RTC Procedure 1	7.0%/5.0 mm	3.1	2.6
RTC Procedure 2	1.3%/0.95 mm	10.9	10.5
RTC Procedure 3	−17.7%/ − 12.6 mm	35.3	40.8
RTC Procedure 4	−0.8%/ − 0.59 mm	18.1	13.9
RTC Procedure 5	−15.7%/ − 11.2 mm	28.1	25.0
RTC Procedure 6	−0.8%/ − 0.59 mm	13.7	13.1

Finally, in the shown case study, it was observed that the augmentation of the RB-RTC with nowcast data leads to a significant decrease in operational performance compared to both the perfect forecast case and the baseline RB-RTC. This is despite the potential of nowcast to decrease the total CSO volume for all analysed procedures.

4.4. Comparative assessment

Of the six RTC procedures presented here, Procedure 1 (relying on the correct prediction at the end of the event to switch off the pumped CSOs) was able to reduce the CSO volume in both the perfect and real nowcast cases. This is consistent with the ability of the nowcast model to predict the end of a rainfall event (as previously shown in Figure 10). Although this accuracy is not perfect (mean SPC of 0.81), the effect of incorrect predictions appears to have a small impact on the UDS operational performance (3% CSO volume increase compared to the perfect baseline).

Conversely, a higher risk of operational deterioration was observed when the RB-RTC procedure sets the CSO pump settings directly dependent on the forcing of the forecasted rainfall depth in a modelled setting. This was further exacerbated by switching on the pumped CSOs if a higher threshold was predicted (using a FD of 0.9 as opposed to 0.8). As these procedures used the entire forecast horizon to predict the depth (with an activation only occurring at the higher end of the rainfall prediction), both rely on two of the weakest points identified in the nowcast data. These are using the direct numerical prediction over the full horizon (120 min) and using a high threshold for the activation of the rules. Procedure 5 relied on a consistent forecast in order to activate, though, as also shown through the nowcast performance assessment, this did not increase the robustness of the control procedure.

The results from the nowcast accuracy assessment yielded similar trends compared to the model-based risk assessment methodology. Although it is not possible to quantify the risks directly from the nowcast data, due to aforementioned non-linearities and the nature of the risks identified here, the statistical analysis of nowcast data gives a strong indication on how the nowcast can be included in future RB-RTC strategies. This, in turn, allows bypassing the extensive model-based analyses, as presented here, and allows operators to make informed decisions based on less data and model outputs.

5. DISCUSSIONS

The maximum potential CSO reduction reported here (14.6% for Procedure 4) is smaller when compared to the corresponding reduction reported by other studies shown in Table 1. However, those studies focussed on the evaluation of either a single detention pond or a stormwater system, i.e. drainage (sub-)systems with a relatively high level of controllability (in terms of the level of influence of actuators on the behaviour of the system). As controllability is one of the key factors influencing RTC efficacy potential (van der Werf *et al.* 2022), it is expected that the optimised functioning improved the system more in the previous studies compared to those reported here. A lack of information on the full RTC potential of the previously reported systems, furthermore, makes the direct comparison impossible.

When comparing the performance loss related to the nowcast accuracy with real-time RTC optimisation procedures, the self-adjusting mechanism reported to reduce the impact (Fiorelli *et al.* 2013; Courdent *et al.* 2015) was not observed in the model-based risk assessment results. This is likely to be a result of the relatively long sampling interval and the design of the updated RB-RTC procedures. However, it is possible that an increased level of risk could be an inherent drawback of

RB-RTC including nowcast compared to real-time optimisation procedures. Additional evidence, based on different case studies following the presented methodology here, is necessary to ascertain the latter and attribute and quantify the relative importance of the former two.

Furthermore, studies which investigate the impact of nowcast uncertainty through synthetic errors (e.g. Svensen *et al.* 2021) are likely to misreport the potential impacts of nowcast uncertainties, given the dynamics observed here. The use of real nowcast algorithms in combination with real observed data is therefore considered to be a must for applicable results.

Although the methodology presented here applies to other case studies, the main findings depend on the available nowcast data (both events within the dataset and the forecast model used to generate the nowcast data) and hence the results obtained in this work may, therefore, not be directly transferable (He *et al.* 2013; Imhoff *et al.* 2020). The nowcast data accuracy assessment, as presented here, should, therefore, be done prior to the implementation of nowcast-included RB-RTC in other case studies to ensure similar dynamics are observed.

With the rise of machine learning (ML) applications in the field of rainfall nowcasting (Ravuri *et al.* 2021; Amini *et al.* 2022), new nowcasting methods which focus on specific rainfall properties (i.e. timing or magnitude of the start of an event, total sum of the horizon or prediction of the ending of the event) could improve the functionality of RB-RTC augmented with nowcast. Similarly, the use of ensemble forecasts has previously been shown to be beneficial in an RTC context (He *et al.* 2013; Courdent *et al.* 2015; Balla *et al.* 2020). Understanding the differences within the ensemble forecast can further decrease potential uncertainties and their effect on the operation of UDS.

It should be noted that the updated RB-RTC procedures were not formally optimised nor designed to be robust against nowcast uncertainties, as the aim of this research was to investigate the effects of nowcast uncertainties on RB-RTC procedures. Furthermore, the prediction of the *end-of-the-event* was particularly useful in the used case study due to the presence of CSO pumps, enabling the direct switching off of these pumps when no rainfall was expected. The applicability of the *end-of-the-event* prediction to other case studies might be more limited.

When implementing nowcast-informed RB-RTC, a detailed trade-off between the added benefits of a longer horizon and the induced uncertainties should be done. Increased horizons have been shown to plateau in their potential for system operative improvement (Jafari *et al.* 2020) and therefore inclusion of the entire horizon, as was done in some of the procedures developed here, might lead to sub-optimal operation.

6. CONCLUSIONS

This research aims to understand how heterogeneity in nowcast accuracy, dependent on varying rainfall properties, can affect and be used in a RB-RTC procedure for the improvement of UDS operation. Using both perfect and real nowcast rainfall data in the Rotterdam UDS, a model-based study was performed to assess the risk of six different RB-RTC procedures potentially resulting in performance loss or operational deterioration of the analysed UDS. Based on the results obtained, the following conclusions could be drawn:

- Multiple forms of nowcast-informed RB-RTC can significantly decrease the pollution load from UDS when using perfect nowcast data. However, significant risks are associated with using real nowcast data to control the UDS resulting, in some cases, in significantly increasing the CSO frequency and volume.
- Nowcast accuracy is heterogeneous and depends on the stage and depth of the rainfall event. The nowcast data indicated a strong predictability of the end of a rainfall event but poor performance at the start and in the middle of an event, particularly when larger rainfall depths were observed.
- This heterogeneity relates directly to risks of operative deterioration and performance loss, as the impact of the uncertainty can be inferred directly from the nowcast data. Using these inferred risks, decisions can be made about the development of nowcast-informed RB-RTC.
- The dynamics related to heuristic control versus real-time optimisation control in the context of uncertain forecasts differ, as the heuristic control does not appear to have a strong self-correcting mechanism. A real-time optimisation strategy might, therefore, be a more robust implementation of nowcast-informed forms of control.

Based on these conclusions, additional research is needed to understand if the results and conclusions drawn from this case study are transferable to other UDSs. Furthermore, the ability to formally optimise the nowcast-informed RB-RTC using real nowcast data was not assessed here and a comparative assessment of a nowcast-informed RB-RTC calibrated on real and perfect data should be done. Additional measures to ensure the resilience of heuristic control to uncertain rainfall data should be investigated.

ACKNOWLEDGEMENTS

The authors would like to thank the Royal Dutch Meteorological Institute (KNMI) for providing the nowcast data used in this paper. Furthermore, the authors also thank Imber Advies for preparing the models used for the design of the control rules and used in the assessment of the framework and the City of Rotterdam for providing the necessary data. This research was carried out through funding of the Kennisprogramma Urban Drainage, which is sponsored through ARCADIS, Deltares, Evides, Gemeente Almere, Gemeente Arnhem, Gemeente Breda, Gemeente 's-Gravehage, Gemeentewerken Rotterdam, Gemeente Utrecht, GMB Rioleringstechniek, KWR Watercycle Research Institute, Royal HaskoningDHV, Stichting Rioned, STOWA, Sweco, Tauw, Vandervalk&deGroot, Waterboard de Dommel, Waternet and Witteveen&Bos. We would like to thank all the partners for their continued support.

AUTHOR CONTRIBUTIONS

J.A.v.d.W. carried out the analysis of the nowcast and schematised the inclusion of forecast in the control strategy. J.G.L. designed the original control strategy and acquired funding for the research. J.A.v.d.W. wrote the initial draft of the manuscript. All the research was carried out under the active supervision of Z.K. and J.G.L. All authors co-edited the final manuscript.

DATA AVAILABILITY STATEMENT

Data cannot be made publicly available; readers should contact the corresponding author for details.

CONFLICT OF INTEREST

The authors declare there is no conflict.

REFERENCES

Achleitner, S., Fach, S., Einfalt, T. & Rauch, W. 2009 Nowcasting of rainfall and of combined sewage flow in urban drainage systems. *Water Science and Technology* **59** (6), 1145–1151. doi:10.2166/WST.2009.098.

Amini, A., Dolatshahi, M. & Kerachian, R. 2022 Adaptive precipitation nowcasting using deep learning and ensemble modeling. *Journal of Hydrology* **612**, 128197.

Ashok, S. P. & Pekkat, S. 2022 A systematic quantitative review on the performance of some of the recent short-term rainfall forecasting techniques. *Journal of Water and Climate Change* **13**, 3004. doi:10.2166/wcc.2022.302.

Balla, K. M., Schou, C., Bendtsen, J. D. & Kallesøe, C. S. 2020 Multi-scenario model predictive control of combined sewer overflows in urban drainage networks. In: *2020 IEEE Conference on Control Technology and Applications (CCTA)*. IEEE, pp. 1–6.

Baumgartner, D. & Kolassa, J. 2021 Power considerations for Kolmogorov-Smirnov and Anderson-Darling two-sample tests. *Communications in Statistics – Simulation and Computation*. doi:10.1080/03610918.2021.1928193.

Beeneken, T., Erbe, V., Messmer, A., Reder, C., Rohlfing, R., Scheer, M., Schuetze, M., Schumacher, B., Weilandt, M. & Weyand, M. 2013 Real time control (RTC) of urban drainage systems – a discussion of the additional efforts compared to conventionally operated systems. *Urban Water Journal*. doi:10.1080/1573062X.2013.790980.

Beersma, J., Hakvoort, H., Jilderda, R., Overeem, A. & Versteeg, R. 2019 *Neerslagstatistiek en -Reeksen Voor het Waterbeheer 2019*. Amersfoort.

Bilodeau, K., Pelletier, G. & Duchesne, S. 2019 Real-time control of stormwater detention basins as an adaptation measure in mid-size cities. *Urban Water Journal* **15** (9), 858–867. doi:10.1080/1573062X.2019.1574844.

Botturi, A., Ozbayram, E. G., Tondera, K., Gilbert, N. I., Rouault, P., Caradot, N., Gutierrez, O., Daneshgar, S., Frison, N., Akyol, Ç., Foglia, A., Eusebi, A. L. & Fatone, F. 2020 Combined sewer overflows: a critical review on best practice and innovative solutions to mitigate impacts on environment and human health. *Critical Reviews in Environmental Science and Technology* **51** (15), 1585–1618. doi:10.1080/10643389.2020.1757957.

Courdent, V. A. T., Vezzaro, L., Mikkelsen, P. S., Mollerup, A. L. & Grum, M. 2015 Using ensemble weather forecast in a risk based real time optimization of urban drainage systems. *La Houille Blanche*. doi:10.1051/lhb/20150025.

European Commission. 2022 *Urban Wastewater Treatment Directive – Revised*. European Commission, Brussels, Belgium.

Fabry, F. & Seed, A. W. 2009 Quantifying and predicting the accuracy of radar-based quantitative precipitation forecasts. *Advances in Water Resources* **32** (7), 1043–1049. doi:10.1016/J.ADVWATRES.2008.10.001.

Fiorelli, D., Schutz, G., Klepiszewski, K., Regneri, M. & Seiffert, S. 2013 Optimised real time operation of a sewer network using a multi-goal objective function. *Urban Water Journal* **10** (5), 342–353. doi:10.1080/1573062X.2013.806560.

Foresti, L., Reyniers, M., Seed, A. & Delobbe, L. 2016 Development and verification of a real-time stochastic precipitation nowcasting system for urban hydrology in Belgium. *Hydrology and Earth System Sciences* **20** (1), 505–527.

Gaborit, E., Muschalla, D., Vallet, B., Vanrolleghem, P. A. & Anctil, F. 2012 Improving the performance of stormwater detention basins by real-time control using rainfall forecasts. *Urban Water Journal*. doi:10.1080/1573062X.2012.726229.

Gaborit, E., Anctil, F., Pelletier, G. & Vanrolleghem, P. A. 2016 Exploring forecast-based management strategies for stormwater detention ponds. *Urban Water Journal* **13** (8), 841–851. doi:10.1080/1573062X.2015.1057172.

García, L., Barreiro-Gomez, J., Escobar, E., Téllez, D., Quijano, N. & Ocampo-Martinez, C. 2015 Modeling and real-time control of urban drainage systems: a review. *Advances in Water Resources* **85**, 120–132.

He, S., Raghavan, S. V., Nguyen, N. S. & Liong, S. Y. 2013 Ensemble rainfall forecasting with numerical weather prediction and radar-based nowcasting models. *Hydrological Processes* **27** (11), 1560–1571. doi:.10.1002/HYP.9254.

Ibrahim, Y. A. 2020 Real-time control algorithm for enhancing operation of network of stormwater management facilities. *Journal of Hydrologic Engineering* **25** (2). doi:10.1061/(ASCE)HE.1943-5584.0001881.

Imhoff, R. O., Brauer, C. C., Overeem, A., Weerts, A. H. & Uijlenhoet, R. 2020 Spatial and temporal evaluation of radar rainfall nowcasting techniques on 1,533 events. *Water Resources Research* **56** (8). doi:10.1029/2019WR026723.

Imhoff, R. O., Brauer, C. C., van Heeringen, K. J., Uijlenhoet, R. & Weerts, A. H. 2022 Large-sample evaluation of radar rainfall nowcasting for flood early warning. *Water Resources Research* **58** (3), e2021WR031591.

Jafari, F., Mousavi, S. J. & Kim, J. H. 2020 Investigation of rainfall forecast system characteristics in real-time optimal operation of urban drainage systems. *Water Resources Management* **34** (5), 1773–1787.

Joo, J., Lee, J., Kim, J. H., Jun, H. & Jo, D. 2013 Inter-event time definition setting procedure for urban drainage systems. *Water* **6** (1), 45–58. doi:10.3390/W6010045.

Langeveld, J. G., Benedetti, L., de Klein, J. J. M., Nopens, I., Amerlinck, Y., van Nieuwenhuijzen, A., Flameling, T., van Zanten, O. & Weijers, S. 2013 Impact-based integrated real-time control for improvement of the Dommel River water quality. *Urban Water Journal*. doi:10.1080/1573062X.2013.820332.

Langeveld, J. G., Liefting, H. J., Schoester, J., Schepers, J. & de Groot, A. C. 2022 Development and implementation of a large-scale real time control system: the Rotterdam case study. In: *Proceedings of the International Conference on Urban Drainage Modelling*, USA.

Lin, C., Vasić, S., Kilambi, A., Turner, B. & Zawadzki, I. 2005 Precipitation forecast skill of numerical weather prediction models and radar nowcasts. *Geophysical Research Letters* **32** (14), 1–4. doi:10.1029/2005GL023451.

Löwe, R., Vezzaro, L., Mikkelsen, P. S., Grum, M. & Madsen. H. 2016 Probabilistic runoff volume forecasting in risk-based optimization for RTC of urban drainage systems. *Environmental Modelling & Software* **80**, 143–158. doi:10.1016/J.ENVSOFT.2016.02.027.

Lund, N. S. V., Falk, A. K. V., Borup, M., Madsen, H. & Mikkelsen, P. S. 2018 Model predictive control of urban drainage systems: a review and perspective towards smart real-time water management. *Critical Reviews in Environmental Science and Technology*. doi:10.1080/10643389.2018.1455484.

Mahaut, V. & Andrieu, H. 2019 Relative influence of urban-development strategies and water management on mixed (separated and combined) sewer overflows in the context of climate change and population growth: a case study in Nantes. *Sustainable Cities and Society* **44**, 171–182. doi:10.1016/J.SCS.2018.09.012.

Marshall, J. S., Hitschfeld, W. & Gunn, K. L. S. 1955 Advances in radar weather. *Advances in Geophysics* **2**, 1 -56. Doi: 10.1016/S0065-2687(08)60310-6.

McDonnell, B. E., Ratliff, K., Tryby, M. E., Wu, J. J. X. & Mullapudi, A. 2020 PySWMM: the python interface to stormwater management model (SWMM). *Journal of Open Source Software* **5** (52), 2292. doi:10.21105/joss.02292.

Mollerup, A. L., Mikkelsen, P. S., Thornberg, D. & Sin, G. 2017 Controlling sewer systems – a critical review based on systems in three EU cities. *Urban Water Journal* **14** (4), 435–442. doi:10.1080/1573062X.2016.1148183.

Naughton, J., Sharior, S., Parolari, A., Strifling, D. & McDonald, W. 2021 Barriers to real-time control of stormwater systems. *Journal of Sustainable Water in the Built Environment* **7** (4). doi:10.1061/JSWBAY.0000961.

Overeem, A., Holleman, I. & Buishand, A. 2009 Derivation of a 10-year radar-based climatology of rainfall. *Journal of Applied Meteorology and Climatology* **48** (7), 1448–1463. doi:10.1175/2009JAMC1954.1.

Owolabi, T. A., Mohandes, S. R. & Zayed, T. 2022 Investigating the impact of sewer overflow on the environment: a comprehensive literature review paper. *Journal of Environmental Management* **301**, 113810. doi:10.1016/J.JENVMAN.2021.113810.

Pichler, M. 2022 Swmm_api: API for reading, manipulating and running SWMM-Projects. doi:10.5281/zenodo.7054804.

Pleau, M., Pelletier, G., Colas, H., Lavallee, P. & Bonin, R. 2001 Global predictive real-time control of Quebec Urban Community's westerly sewer network. *Water Science and Technology* **43** (7), pp. 123–130. doi: 10.2166/wst.2001.0404

Pulkkinen, S., Chandrasekar, V., von Lerber, A. & Harri, A.-M. 2020 Nowcasting of convective rainfall using volumetric radar observations. *IEEE Transactions on Geoscience and Remote Sensing* **58** (11), 7845–7859.

Ravuri, S., Lenc, K., Willson, M., Kangin, D., Lam, R., Mirowski, P., Fitzsimons, M., Athanassiadou, M., Kashem, S., Madge, S., Prudden, R., Mandhane, A., Clark, A., Brock, A., Simonyan, K., Hadsell, R., Robinson, N., Clancy, E., Arribas, A. & Mohamed, S. 2021 Skilful precipitation nowcasting using deep generative models of radar. *Nature* **672**, 597. doi:10.1038/s41586-021-03854-z.

Rossman, L. A. 2015 *Storm Water Management Model User's Manual*. National Risk Management Research Laboratory, Office of Research and Development, U.S. Environmental Protection Agency, Cincinnati.

Schellart, A., Liguori, S., Krämer, S., Saul, A. & Rico-Ramirez, M. A. 2014 Comparing quantitative precipitation forecast methods for prediction of sewer flows in a small urban area. *Hydrological Sciences Journal* **59** (7), 1418–1436. doi:10.1080/02626667.2014.920505.

Schütze, M., Campisano, A., Colas, H., Schilling, W. & Vanrolleghem, P. A. 2002 Real-time control of urban wastewater systems – where do we stand today? In: Strecker, E. W. & Huber, W. C. (eds). *Global Solutions for Urban Drainage*. ASCE, Portland, Oregon, USA, pp. 1–17.

Svensen, J. L., Sun, C., Cembrano, G. & Puig, V. 2021 Chance-constrained stochastic MPC of Astlingen urban drainage benchmark network. *Control Engineering Practice* **115**, 104900. doi:10.1016/J.CONENGPRAC.2021.104900.

ten Veldhuis, J. A. E., Clemens, F. H. L. R., Sterk, G. & Berends, B. R. 2010 Microbial risks associated with exposure to pathogens in contaminated urban flood water. *Water Research* **44** (9), 2910–2918.

Tian, W., Liao, Z., Zhi, G., Zhang, Z. & Wang, X. 2022 Combined sewer overflow and flooding mitigation through a reliable real-time control based on multi-reinforcement learning and model predictive control. *Water Resources Research* **58** (7), e2021WR030703.

van Daal, P., Gruber, G., Langeveld, J., Muschalla, D. & Clemens, F. 2017 Performance evaluation of real time control in urban wastewater systems in practice: review and perspective. *Environmental Modelling & Software* **95**, 90–101.

van der Werf, J. A., Kapelan, Z. & Langeveld, J. 2021 Quantifying the true potential of real time control in urban drainage systems. *Urban Water Journal* **18** (10), 873–884. doi:10.1080/1573062X.2021.1943460.

van der Werf, J. A., Kapelan, Z. & Langeveld, J. 2022 Towards the long term implementation of real time control of combined sewer systems: a review of performance and influencing factors. *Water Science and Technology* **85** (4). doi:10.2166/wst.2022.038.

van der Werf, J. A., Kapelan, Z. & Langeveld, J. 2023 Real-time control of combined sewer systems: risks associated with uncertainties. *Journal of Hydrology* **617**, 128900. doi:10.1016/J.JHYDROL.2022.128900.

Vezzaro, L. 2021 Extrapolating performance indicators for annual overflow volume reduction of system-wide real time control strategies. *Urban Water Journal* **19** (1), 15–21. doi:10.1080/1573062X.2021.1948078.

Vezzaro, L. & Grum, M. 2014 A generalised dynamic overflow risk assessment (DORA) for real time control of urban drainage systems. *Journal of Hydrology* **515**, 292–303. doi:10.1016/J.JHYDROL.2014.05.019.

First received 5 December 2022; accepted in revised form 20 January 2023. Available online 1 February 2023